Available online at www.sciencedirect.com
ScienceDirect
Trans. Nonferrous Met. Soc. China 24(2014) 3378−3385
Transactions of Nonferrous Metals Society of China
www.tnmsc.cn

Non-isothermal kinetic analysis of thermal dehydration of $La_2(CO_3)_3·3.4H_2O$ in air

Xiang-hui ZHANG[1], Chuan HE[2], Ling WANG[1], Jing LIU[1], Miao DENG[1], Qian FENG[3]

1. College of Materials and Chemistry and Chemical Engineering, Chengdu University of Technology, Chengdu 610059, China;
2. College of Mechanical and Electrical Engineering, Central South University, Changsha 410012, China;
3. NETZSCH Scientific Instrument Trading Co., Ltd., Chengdu Branch, Chengdu 610017, China

Received 12 September 2013; accepted 14 November 2013

Abstract: The single phase $La_2(CO_3)_3·3.4H_2O$ was synthesized by hydrothermal method. The thermal decomposition and intermediates and final solid products of $La_2(CO_3)_3·3.4H_2O$ from 30 to 1000 °C were characterized by XRD, FTIR and DTA−TG. The kinetics of dehydration of $La_2(CO_3)_3·3.4H_2O$ in the temperature range of 30−366 °C was investigated under non-isothermal conditions. Flynn−Wall−Ozawa and Friedman isoconversion methods were used to calculate the activation energy and analyze the reaction steps; multivariate non-linear regression program was applied to determine the most probable mechanism and the kinetic parameters. The results show that the thermal dehydration of $La_2(CO_3)_3·3.4H_2O$ is a kind of three-step competitive reaction, and controlled by an *n*-order initial reaction followed by *n*-order competitive reaction ($F_nF_nF_n$ model). The activation energy matching with the most probable model is close to value obtained by Friedman method. The fitting curves match the original TG−DTG curves very well.

Key words: $La_2(CO_3)_3·3.4H_2O$; non-isothermal kinetics; simultaneous thermal analysis; dehydration reaction

1 Introduction

Rare earth metal compounds, particularly lanthanum, cerium, and yttrium, are formed as porous particles and are effective in binding metals, metal ions, and phosphate [1]. These compounds may be used in the gastrointestinal tract or the bloodstream to remove phosphate or to treat hyperphosphatemia in mammals [2]. Now, certain forms of lanthanum carbonate hydrate as an effective and safe non-calcium, non-aluminum oral phosphate binder, have been used to treat hyperphosphataemia in patients with renal failure [3]. Lanthanum carbonate hydrate has the formula $La_2(CO_3)_3·xH_2O$, where x has a value between 0 and 10 [4]. Several studies show that hydrated lanthanum carbonates with about 3 to 4 molecules of crystal water provide the highest removal rate of phosphate [1,2]. Thus, it is highly important to understand the characteristics and dehydration mechanism of hydrated lanthanum carbonates; especially with 3 to 4 molecules of crystal water, it would be useful for the synthesis and medicinal application of the material. Kinetic analysis of the dehydration reactions by thermal analysis technique can be used to evaluate the optimum conditions in industrial production.

To date, considerable work has been focused on the preparation of the hydrated lanthanum carbonates with different molecules of crystal water like $La_2(CO_3)_3·8H_2O$ [5], $La_2(CO_3)_3·6H_2O$ [1], $La_2(CO_3)_3·4H_2O$ [6], $La_2(CO_3)_3·1.7H_2O$ [7], $La_2(CO_3)_3·1.4H_2O$ [5]. The decomposition of the hydrated lanthanum carbonates has also been investigated extensively using SEM, XRD, thermal analysis and FTIR techniques [1−7]. These works show that more intermediate products were involved besides those reported $La_2(CO_3)_3$, $La_2O_2(CO_3)$ and La_2O_3. Unfortunately, most literatures rested on the preparation and thermal decomposition process of

Foundation item: Project (201011005-5) supported by the National Land and Resources Public Welfare Scientific Research Project of China; Project (41030426) supported by the National Natural Science Foundation of China; Project (20095122110015) supported by Specialized Research Fund for the Doctoral Program of Higher Education of China; Project (2010-32) supported by Scientific Research Foundation of the Education Ministry for Returned Chinese Scholars, China

Corresponding author: Ling WANG; Tel: +86-28-84076198; Fax: +86-28-84079074; E-mail: wangling@cdut.edu.cn

DOI: 10.1016/S1003-6326(14)63480-4

hydrated lanthanum carbonates and few attention was paid to the kinetics and the most probable model of thermal dehydration.

The aim of this work is, therefore, to study the thermal dehydration kinetics of as-prepared pure lanthanum carbonate hydrate. Kinetic data were collected by simultaneous thermal analysis technique. Non-isothermal kinetic analyses were employed by using Netzsch thermokinetics software.

2 Experimental

2.1 Preparation of lanthanum carbonate hydrate

25 g of lanthanum chloride was added to 100 mL deionized water and then stirred for 15 min at 25−35 °C. The solution was filtered through a funnel and flask under vacuum. 316 g of ammonium bicarbonate was added to 2000 mL deionized water. The ammonium bicarbonate filtrate was added slowly in 3−4 h into lanthanum chloride solution. The pH value of mixture solution was adjusted in the range of 3−4 by adding ammonium bicarbonate during reaction. After the completion of reaction, deionized water was added to the mixed solution and maintained at 25−35 °C for 3−4 h. The reaction products were filtered under vacuum and washed with deionized water repeatedly to get rid of the chlorides. The wet material was dried in an oven for 3−4 h.

2.2 Characterization of lanthanum carbonate hydrate

A Netzsch STA409PC simultaneous thermal analyzer was used for thermogravimetry (TG) and differential thermal analysis (DTA) with different scanning rates (5, 10, 15, 20 K/min) from 30 to 1000 °C. An alumina crucible container was used in air. The gas flow rate was 30 mL/min. Sample mass was around 12 mg. The decomposition products were collected at the temperatures shown on the DTA−TG curves. Prior to experiments, temperature calibration was performed. All experiments were performed twice to show the reproducibility. The thermokinetic calculation was conducted with the help of NETZSCH thermokinetic software, using the detected TG data.

The X-ray diffraction (XRD) pattern of each sample was obtained using a Rigaku D/MAX-ⅢC powder diffractometer. The X-ray generator was equipped with a Ni filter and generated a beam of Cu K_α radiation (λ=0.15418 nm). The operational settings for all the XRD scans were voltage of 40 kV, current of 30 mA, 2θ range of 10°−70°, scanning speed of 0.6 (°)/s.

Fourier transform infrared (FTIR) spectra were obtained at a resolution of 4 cm^{-1}, over the range 4000−600 cm^{-1}, using a Bruker Tensor 27 spectrophotometer with KBr pellets.

3 Results and discussion

3.1 Characterization of as-prepared products

The XRD pattern and IR spectrum of the as-prepared products are given in Fig. 1. The XRD pattern shows that all the diffraction peaks in the pattern are in agreement with those of the orthorhombic type of $La_2(CO_3)_3·4H_2O$, with space group *Pmp*21(18) and lattice constants *a*=9.57 Å, *b*=12.65 Å, and *c*=8.94 Å (standard card JCPD No. 06−0076). The strong diffraction peak at 2θ=13.528° is attributed to the layered structure of $La_2(CO_3)_3·4H_2O$ [8]. No diffraction peaks of impurities are observed.

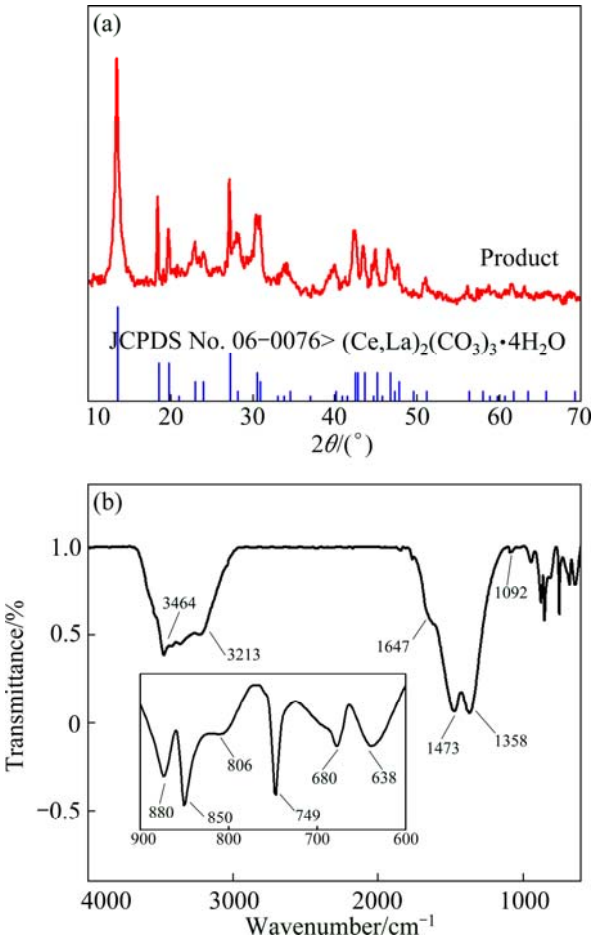

Fig. 1 XRD pattern (a) and IR spectrum (b) of as-prepared products

The IR spectrum shows the main bands at 3464 and 1647 cm^{-1} are due to lattice water vibration and the carbonate anion at 1092 cm^{-1} (symmetric stretching), 1473 and 1357 cm^{-1} (asymmetric stretching), 749 cm^{-1} (symmetric bending), (asymmetric bending) at 880, 850, 806 cm^{-1} [8−10]. The two main bands at 638 and 680 cm^{-1} are due to lattice vibration of La−O [11]. ZHANG et al [9] conducted the FTIR measurement on

$La_2(CO_3)_3·8H_2O$, $La_2(CO_3)_3·3.3H_2O$ and $La(OH)CO_3$. They have shown that the IR spectrum characteristic peaks of the $La_2(CO_3)_3·3.3H_2O$ were at 849, 747, 681 cm^{-1}, rather than at 858, 724, 696 cm^{-1}, for the lanthanum hydroxycarbonate ($La(OH)CO_3$), which is similar to that in the present study, and indicates that no impurities like $La(OH)CO_3$ exist in the as-prepared products. Hence, the single-phase approximate $La_2(CO_3)_3·4H_2O$ composition was prepared successfully.

3.2 Thermal decomposition process

Figure 2 shows the DTA−TG−DTG curves of the as-prepared products at a heating rate of 10 K/min in air below 1000 °C. The thermal decomposition of the as-prepared products occurs in four steps in accordance with the DTG peaks, and all steps are endothermic reaction.

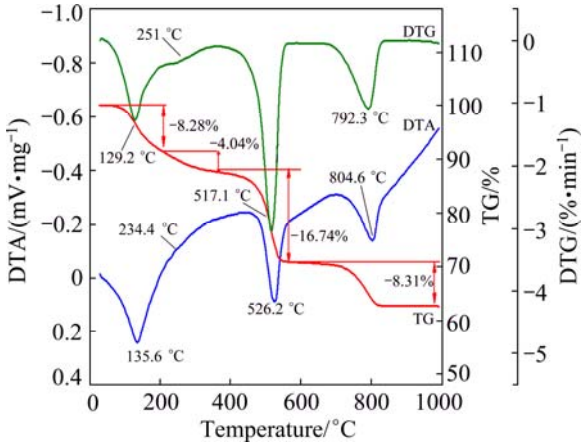

Fig. 2 DTA−TG−DTG curves of as-prepared product at heating rate of 10 K/min in air

The first step and the second step are from 30 to 202 °C (mass loss of 8.28%, t_{max}=135.6 °C) and 202 to 366 °C (mass loss of 4.04%, t_{max}=234.4 °C), respectively, with an overall mass loss of 12.34%, which is in good agreement with the calculated mass loss of 12.32%, attributed to the evaporation of 3.4 mol H_2O of crystallization in the as-prepared lanthanum carbonate hydrate and the formation of anhydrous $La_2(CO_3)_3$. The results obtained by the TG analysis confirm that the compound of the as-prepared product is $La_2(CO_3)_3·3.4H_2O$.

The IR spectrum of the intermediates heated at 130 °C (Fig. 3) shows a great deal of similarity to that of the unheated $La_2(CO_3)_3·3.4H_2O$, because both of them show absorption bands arising from carbonate anions (at 1750−640 cm^{-1}) and water of hydration (at 3440 and 1640 cm^{-1}) [8,10]. The IR spectra from 168 to 360 °C (Fig. 3) show that the CO_3^{2-} species become strong between 1000 and 600 cm^{-1}, and the absorptions band at 2345 cm^{-1} begin to appear [8]. However, the lattice water

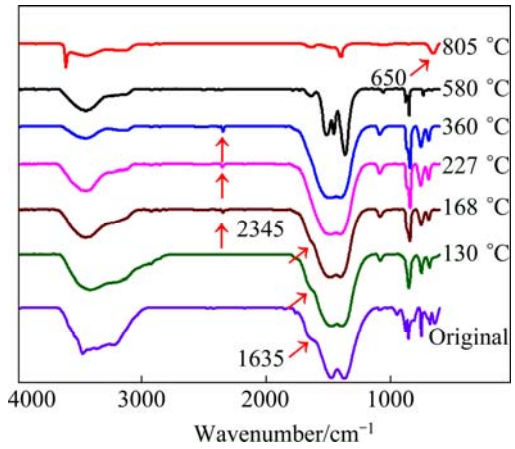

Fig. 3 IR spectra in range of 400−600 cm^{-1} of as-prepared products heated at different temperatures

vibration at 1635 cm^{-1} disappears up to 227 °C. The corresponding XRD pattern (Fig. 4(a)) indicates that at 130 °C, the intensity of the characteristic diffraction peaks of the as-prepared products (Fig. 1) decreases very fast, and the products become poorly crystallized. Between 168 and 360 °C, the characteristic diffraction peaks of the products almost disappear except 2θ=18.4°, and the products are amorphous [12]. The peak at 2θ=18.4° corresponds to (020) plane in the orthorhombic structure [8], which is a layered structure with lanthanum and carbonate ions forming planes which are separated by planes of water molecules [13]. The results obtained by the FTIR and XRD analyses confirm that the lanthanite structure does not completely collapse during the dehydration process [12,13].

The third step is from 366 to 566 °C (mass loss of 16.74%, t_{max}=526.2 °C), which can be assigned to the decomposition of $La_2(CO_3)_3$ into dioxycarbonate, $La_2O_2CO_3$. The corresponding IR spectrum and XRD pattern support the reaction process. The IR spectrum at 580 °C shows a strong absorption between 1600 and 1300 cm^{-1} and also at 1060 and 870 cm^{-1} assignable to oxycarbonate species [10], and a diffraction pattern of pure well-crystallized $La_2O_2CO_3$ (standard card JCPD No. 48−1113) is observed in Fig. 4(b).

The fourth step is from 566 to 1000 °C (mass loss of 8.31%, t_{max}=792.3 °C), which accounts for the conversion of $La_2O_2CO_3$ to La_2O_3. It can be seen from the FTIR spectrum of 805 °C that the characteristic absorbance band at about 650 cm^{-1} is the La−O stretching vibration [11]. The weak bands around 3610, 1600 and 1500 cm^{-1} are most probably due to surface contamination by carbonate and moisture [14]. The corresponding XRD pattern of pure La_2O_3 (standard card JCPD No.05−0602) is observed in Fig. 4(c).

Studies on the thermal behavior of the as-prepared $La_2(CO_3)_3·3.4H_2O$ showed features in agreement with the

others observed for other lanthanum carbonates such as $La_2(CO_3)_3·8H_2O$, $La_2(CO_3)_3·1.4H_2O$, $La_2(CO_3)_3$, $La_2(CO_3)_2(OH)_2·H_2O$ [7]. All data are listed in Table 1, where the experimental values are consistent with the theoretical values for all steps. Based on XRD, FTIR, TG and DTA analyses, the following pattern is proposed for decomposition of the as-prepared $La_2(CO_3)_3·3.4H_2O$:

$$La_2(CO_3)_3\cdot 3.4H_2O \xrightarrow{135.6\,^\circ C}$$
$$La_2(CO_3)_3\cdot 1.1H_2O \xrightarrow{234.4\,^\circ C} La_2(CO_3)_3 \xrightarrow{526.2\,^\circ C}$$
$$La_2O_2CO_3 \xrightarrow{804.6\,^\circ C} La_2O_3$$

Figure 5 shows TG and DTG curves of the thermal dehydration of $La_2(CO_3)_3·3.4H_2O$ at four heating rates over the temperature range of 30−366 °C. It can be seen that all the samples show similar TG and DTG curves. The mass loss is dependent of the heating rate, since the mass loss decreases with increasing heating rate. DTG curves of all the samples have two peaks; with the increase of heating rate, the maximum temperature of the peak (T_p) shift to higher temperature. This implies that the dehydration occurs in at least two steps of a complex reaction path.

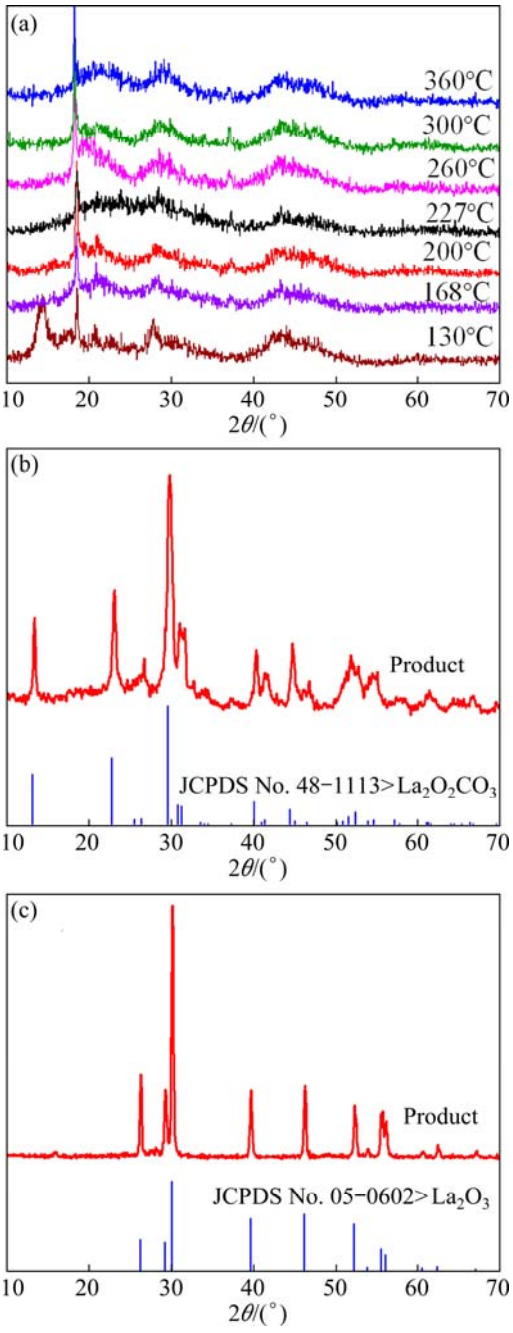

Fig. 4 XRD patterns of as-prepared products heated at different temperatures: (a) 130−360 °C; (b) 580 °C; (c) 805 °C

Table 1 Comparison of experimental and calculated mass change with an approximate composition of $La_2(CO_3)_3·3.4H_2O$ in air (10 K/min)

Step	Temperature/ °C	Mass change/%		Solid product
		Exp.	Calc.	
1	30−202	−8.28	−8.33	$La_2(CO_3)_3·1.1H_2O$
2	202−366	−4.04	−3.99	$La_2(CO_3)_3$
3	366−566	−16.74	−16.61	$La_2O_2CO_3$
4	566−1000	−8.31	−8.31	La_2O_3

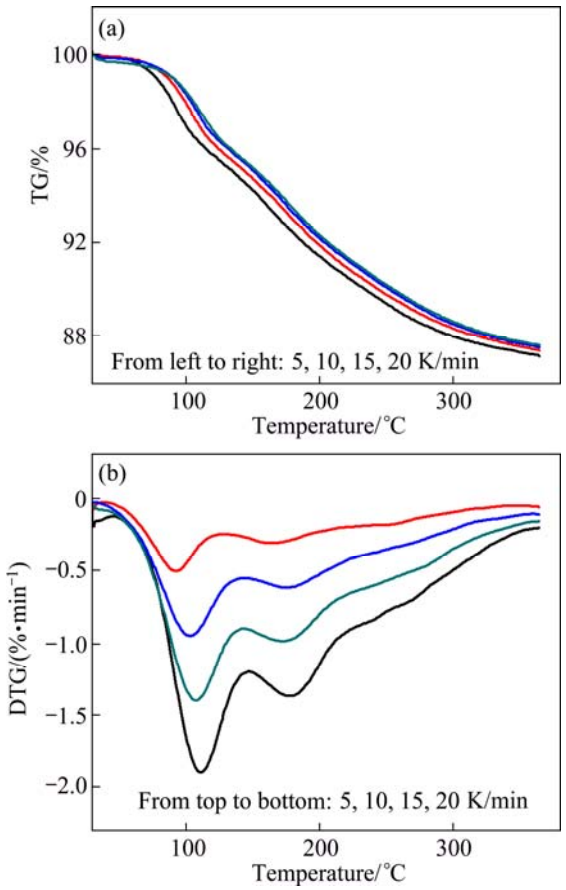

Fig. 5 TG and DTG curves of $La_2(CO_3)_3·3.4H_2O$ at different heating rates from 30 to 366 °C: (a) TG curves; (b) DTG curves

3.3 Non-isothermal kinetics

3.3.1 Estimation of activation energy *E* of dehydration

For the solid-state non-isothermal decomposition

reactions, the reactions rate is expressed by [15]

$$d\alpha/dT=(A/\beta)\exp[(-E/(RT)]f(\alpha) \quad (1)$$

where T is the temperature; α is the reaction rate constant; β is the linear heating rate; $f(\alpha)$ is the reaction mechanism function; A is the frequency factor; E is the activation energy; R is the mole gas constant. The purpose of this work is to obtain the three factors of the above equations, i.e., E, A, and $f(\alpha)$.

1) Flynn−Wall−Ozawa (FWO) method [16]

Equation (2) shows FWO method which follows logarithmic form of Eq. (1).

$$\ln\ \beta=\lg[AE/Rf(\alpha)]-2.315-0.456E/(RT) \quad (2)$$

In terms of the FWO method, the slope of ln β vs $1/T$ for the same value of α gives the value of E, and A can be calculated by intercept when $f(\alpha)$ is coincident.

2) Friedman−Reich−Levi (FRL) method [17]

By integration of Eq. (1), FRL method is obtained:

$$\ln[\beta(d\alpha/dT)]=\ln[Af(\alpha)]-E/(RT) \quad (3)$$

In accordance with the FRL method equation, the slope of $\ln[\beta(d\alpha/dT)]$ vs $1/T$ for the same value of α gives the value of E, and A can be calculated by intercept when $f(\alpha)$ is coincident.

By replacing the values of α, β, T into Eqs. (2) and (3), the results based on the TG data by the FRL and FWO methods are shown in Fig. 6. It can be seen that lg $[\beta(d\alpha/dT)]$ and lg β both change with $1/T$, which is an indication of the dehydration process of a complex reaction path. In the FRL analysis given in Fig. 6(a), a good separation of the three reaction steps is demonstrated, and the mass loss decreases with increasing heating rate from 30 to 360 °C, indicating that the reaction process includes at least three steps and the presence of a competitive reaction [18].

FWO and FRL methods have a huge advantage, namely, it can provide information on kinetic parameters, such as the activation energy and preexponential factor, without determining a concrete kinetic model [19]. The values of activation energy determined by FRL and FWO methods are comparatively shown in Fig. 7. The values of the E obtained by these two methods are very similar and reasonable. In such cases, the Friedman (FRL) method, which uses directly the equation of reaction rate, is recommended [20]. If E is independent of α, the decomposition may be a simple reaction; otherwise, it is of multistep reaction mechanism [16]. According to the characteristics of the $E-\alpha$ plot of FRL methods, three activation energies can be identified: 85, 115, 193 kJ/mol, corresponding to different conversion degrees α, 0.02, 0.4 and 0.7. So, a three-step kinetic scheme should be employed.

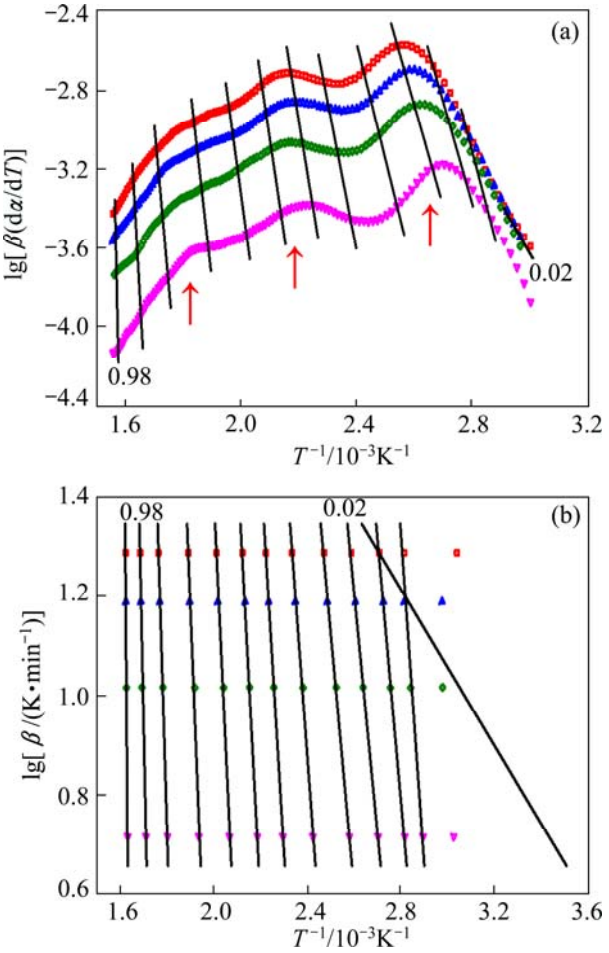

Fig. 6 Analyses of thermal decomposition of $La_2(CO_3)\cdot 3.4H_2O$ by FRL (a) and FWO (b) methods

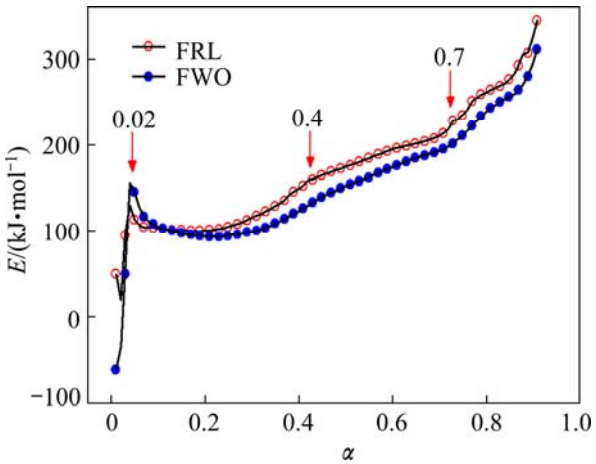

Fig. 7 Activation energies as function of conversion degree α ($0.01\leq\alpha\leq0.91$) by FRL and FWO methods

3.3.2 Determination of most probable mechanism

Based on the analysis of the results of the activation energy by isonversional methods as well as the shape of profiles and isoconversional lines from FWO and FRL plots (Fig. 6), multivariate non-linear regression (Netzsch thermokinetics) was applied to determining the

most probable kinetic model of thermal degradation of the samples. The non-isothermal data recorded at the above mentioned four heating rates were brought together during analysis. The relevant differential equations of the reaction rates were numerically solved. The kinetic parameters were iteratively optimized. The activation energies calculated by FRL method acted as initial values for multivariate non-linear regression process. The degree of the best fitting was determined with the use of the value F_{exp} [18] and regression coefficient. The following schemes (mechanisms) of process were also taken into account:

Scheme coded by t:f,f: $A \xrightarrow{1} B \xrightarrow{2} C \xrightarrow{3} D$;

t:f,c: $A \xrightarrow{1} B \begin{matrix}\xrightarrow{2} C \\ \xrightarrow{3} D\end{matrix}$; t:t,p: $A \xrightarrow{1} B \begin{matrix}\xrightarrow{2} C \\ \xrightarrow{3} C\end{matrix}$

According to the results listed in Table 2 tested by multivariate non-linear regression statistics, the best fit quality was obtained for the schemes coded by t:f,c with the conversion functions F_n–F_n–F_n with the highest correlation coefficient (0.999936) and the F_{exp} does not exceed the critical value (F_{crit}) [18].

The plots of multivariate nonlinear regression based on the TG, DTG data with the best model are presented in Fig. 8. It is seen that there is a good agreement among all the experimental and calculated DTG and TG curves. The results were satisfied.

The corresponding kinetic parameters are listed in Table 3. The dehydration of the as-prepared $La_2(CO_3)_3 \cdot 3.4H_2O$ is controlled by three-step competitive mechanism, an *n*-order initial reaction followed by

Table 2 Results of *F*-test on fit-quality of different models obtained by nonlinear regression

No.	Model code	Scheme	F_{exp}	F_{crit}	Correlation coefficient	Type 1	Type 2	Type 3
1	t:f,c	$A \xrightarrow{1} B \begin{matrix}\xrightarrow{2} C \\ \xrightarrow{3} D\end{matrix}$	1.00	1.16	0.999936	F_n	F_n	F_n
2	t:f,f	$A \xrightarrow{1} B \xrightarrow{2} C \xrightarrow{3} D$	1.21	1.16	0.997651	F_n	F_n	F_n
3	t:f,f		1.22	1.16	0.992223	D_3	D_3	F_n
4	t:f,p	$A \xrightarrow{1} B \begin{matrix}\xrightarrow{2} C \\ \xrightarrow{3} C\end{matrix}$	1.33	1.16	0.997417	F_n	F_n	F_n
5	t:f,p		1.71	1.16	0.995846	F_n	F_n	D_3
6	t:f,f	$A \xrightarrow{1} B \xrightarrow{2} C \xrightarrow{3} D$	1.71	1.16	0.993956	F_n	D_3	D_3
7	t:f,c	$A \xrightarrow{1} B \begin{matrix}\xrightarrow{2} C \\ \xrightarrow{3} D\end{matrix}$	2.12	1.16	0.995889	F_n	F_n	D_3
8	t:f,f	$A \xrightarrow{1} B \xrightarrow{2} C \xrightarrow{3} D$	3.26	1.16	0.974314	D_3	D_3	D_3

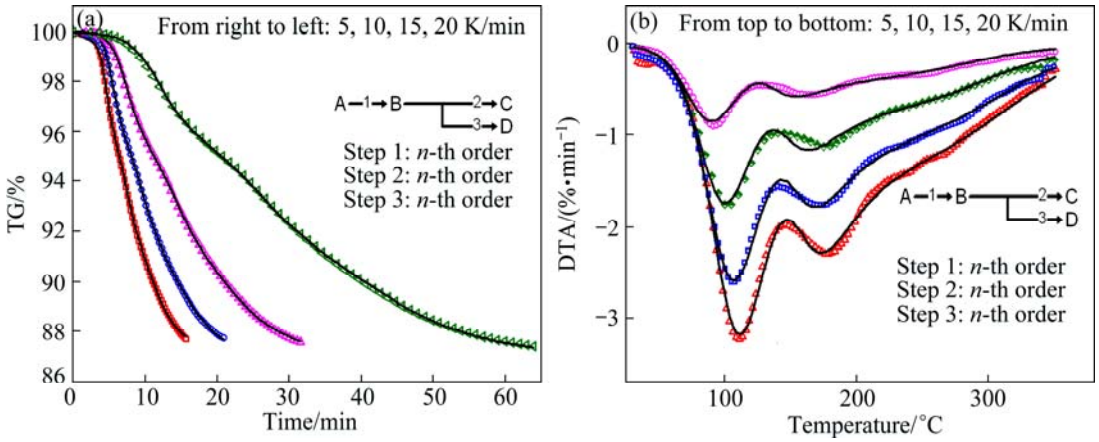

Fig. 8 Multivariate nonlinear regression results through three step method t:f,c (solid line−fitted; symbols−experimental)

Table 3 Non-isothermal kinetic and statistic parameters after non-linear regression through t:f,c model

Step	Function	E/(kJ·mol^{-1})	lg(A/s^{-1})	Parameter	Reaction parameter
1	F_n	85.1192	9.9720	n=5.3881	Foll.React.1=0.8046
2	F_n	146.3906	14.6040	n=3.6967	Comp.React.2=7.6070
3	F_n	195.069	22.2883	n=6.8553	Comp.React.3=0.91864
Fit quality	Correlation coefficient: 0.999936; t-value (α=0.95,492): 1.95593; Durbin-Watson factor: 5.49069				

n-order competitive reaction. As the first step, E=85.12 kJ/mol, $\lg(A/s^{-1})$=9.97, n=5.39; at the second step, E=146.39 kJ/mol, $\lg(A/s^{-1})$=14.60, n=3.697; at the third step, E=195.07 kJ/mol, $\lg(A/s^{-1})$=22.29, n=6.86. It can be seen that the E values matching with the most probable kinetic model are close to the values obtained by FRL methods. ZHANG et al [21] carried out a non-isothermal thermal decomposition kinetics study on lanthanum oxalate decahydrate, and concluded that the activation energies of the first and second step were 65.47 and 110.69 kJ/mol, respectively. BALBOUL et al [14] also conducted the non-isothermal studies on the decomposition course of lanthanum oxalate decahydrate. They have shown that the activation energy was 41−60 kJ/mol from 86 to 225 °C, and 108 kJ/mol at 360 °C. The activation energies determined in the present study are higher than those reported.

In addition, the activation energy listed in Table 3 gradually increases with the dehydration reaction degree. At the first step, the activation energy is similar to the energy for the release of the water of crystallization in the range of 60−80 kJ/mol [21,22]. At the second step, the activation energy is in agreement with the energy for the coordinately bounded decomposition within the range of 130−160 kJ/mol [23,24]. At the third step, the energy is much higher than this range. We attempted to explain the reason that the binding strengths of H_2O molecules in the crystal lattice are different, which results in the differences of reaction temperatures and kinetic parameters [23,24]. The partial H_2O molecules are easily removed to current local place firstly, such as the crystal defect, and accompanied by a density increase with overall increase in close packing. The residual water molecules removal will be more difficult in the more densely packed structures of the lower hydrates, and those residual water molecules are more strongly linked to the non-volatile crystal constituents than to each other [25], which would mean that higher energy is needed to remove the residual water molecules, and the reaction mechanism is controlled by the competitive model rather than by a consecutive model.

4 Conclusions

1) The single-phase $La_2(CO_3)_3\cdot 3.4H_2O$ with the orthorhombic type was successfully prepared by the hydrothermal method. The thermal decomposition process of $La_2(CO_3)_3\cdot 3.4H_2O$ from 30 to 1000 °C undergoes four stages: a two-step dehydration, formation of the dioxycarbonate, and the oxide La_2O_3.

2) The dehydration mechanism of $La_2(CO_3)_3\cdot 3.4H_2O$ in the temperature range 30−366 °C is a kind of three-step competitive reaction. The most probable mechanism was obtained for the schemes coded by t:f,c with the conversion functions $F_nF_nF_n$.

3) The dehydration reaction is controlled by an *n*-order initial reaction followed by *n*-order competitive reaction. At the first step, E=85.12 kJ/mol, $\lg(A/s^{-1})$=9.97, n=5.39; at the second step, E=146.39 kJ/mol, $\lg(A/s^{-1})$=14.60, n=3.697; at the third step, E=195.07 kJ/mol, $\lg(A/s^{-1})$=22.29, n=6.86, Foll.React.1=0.80, Comp.React.2=7.61, Comp.React.3=0.92.

References

[1] NAGARAJ A, INDU E, KUMAR J, SUBHASH G, GNANADEVA G, EALAKRISHNAN C, SUBRAMANIAN I, MANOJ P K, RAJESHS G. Lanthanum composition: USA, US 0020456A1 [P]. 2011−01−27.

[2] MRUDI E, TIMOTHY M S, EDWARD A S, PROCHAZKA J. Rare earth metal compounds, methods of making, and mehods of using the same: USA, US 20110318410A1 [P]. 2011−09−09.

[3] ALBAAJ F, HUTCHISON A J. Lanthanum carbonate (Fosrenol ®): A novel agent for the treatment of hyperphosphataemia in renal failure and dialysis patients [J]. Int J Clin Pract, 2005, 59(9): 1091−1096.

[4] JOSEPHINE C F, PETET N D. Stabilized lanthanum carbonate composition: USA, US 0187602A1 [P]. 2008−04−09.

[5] PANCHULA M L, AKINC M. Morphology of lanthanum carbonate particles prepared by homogeneous precipitation [J]. J Eur Ceram Soc, 1996, 16(8): 833−841.

[6] DONALD H, SIMON G. Method of use for lanthanum carbonate and lanthanum hydroxycarbonate: USA, US 0089948A1 [P]. 2008−04−17.

[7] MASOUD S N, GHADER H, FATEMEH D. Synthesis of lanthanum carbonate nanoparticles via sonochemical method for preparation of lanthanum hydroxide and lanthanum oxide nanoparticles [J]. J Alloys Compd, 2011, 509(1): 134−140.

[8] EBROWN M, DOLLIMORE D, GALWEY A K, BAMFORD C H, HTIPPER C F. Chemical kinetics, reaction in the solid state [M]. Amsterdam: Elsevier, 1980.

[9] ZHANG Ying, HE An-qi, YANG Bo, YE Fang, LING Yang, BAI Xiang, LI Qing, SHUN Yan, LING Zi-huang, WEI Yong-ju, LIU Chui-ge, XU Yi-zhuang, WU Jing-guang. A preparation method of lanthanum carbonate hydrate and judgement method of whether mixed lanthanum hydroxycarbonate: China, CN102442692A [P]. 2012−10−28. (in Chinese)

[10] NAKAMOTO K. Infrared and Raman spectra of inorganic and coordination compounds [M]. New Jersey: Johny Wiley & Sons Inc, 2009.

[11] MASOUD S N, NOSHIN M, GHADER H, FATEMEH D. A novel precursor in preparation and characterization of nickel oxide nanoparticles via thermal decomposition approach [J]. J Alloys Compd, 2010, 493(1−2): 163−168.

[12] MIYAWAKI R, KURIYAMA J, NAKAI I. The redefinition of tengerite-(Y),$Y_2(CO_3)_3\cdot 2{-}3H_2O$, and its crystal structure [J]. Am Mineralist, 1993, 78: 425−432.

[13] SIMON A T R. Structural variations in carbonates [J]. Reviews in Mineralogy and Geochemistry, 2000, 41: 289−308.

[14] BALBOUL B B A, EI-ROUDI A M, SAMIR E, OTHMAN A G. Non-isothermal studies of the decomposition course of lanthanum oxalate decahydrate [J]. Thermochim Acta, 2002, 387(2): 109−114.

[15] VYAZOVKINA S, BURNHAM A K, CRIADO J M, PÉREZ-MAQUEDO L A, POPESCU C, SBIRRAZZUOLI N. ICTAC Kinetics Committee recommendations for performing kinetic computations on thermal analysis data [J]. Thermochim Acta, 2011, 520(1−2): 1−19.

[16] FLYNN J H. A general differential technique for the determination of parameters for d(α)/dt=f(α)Aexp(−E/RT) [J]. J Therm Anal Cal, 1991, 37(2): 293−305.
[17] VLASE T, VLASE G, DOCA M, DOCA N. Specificity of decomposition of solids in non-isothermal conditions [J]. J Therm Anal Cal, 2003, 72(2): 597−604.
[18] OPFERMANN J, BLUMM J. Simulation of the sintering behavior of a ceramic green body using advanced thermokinetic analysis [J]. Thermochim Acta, 1998, 318(1−2): 213−220.
[19] OZAWA T. Kinetic analysis by repeated temperature scanning, Part 1: Theory and methods [J]. Thermochim Acta, 2000, 356(1−2): 173−180.
[20] BUDRUGEAC P, SEGAL E. Some methodological problems concerning nonisothermal kinetic analysis of heterogeneous solid-gas reactions [J]. Int J Chem Kinet, 2001, 33(10): 564−573.
[21] ZHANG Guang, YU Jun-xia, XU Zhi-gao, ZHOU Fang, CHI Ru-an. Kinetics of thermal decomposition of lanthanum oxalate hydrate [J]. Transactions of Nonferrous Metals Society of China, 2012, 22(4): 925−934.
[22] VLAEV L T, NIKOLOVA M M, GOSPODINOV G G. Non-isotherm kinetics of dehydration of some selenite hexahydrates [J]. J Sol State Chem, 2004, 177(8): 2663−2669.
[23] CRIADO J M, PÈREZ-MAQUEDA L A, SĂNCHEZ-JIMNEZ P E. Dependence of the preexponential factor on temperature [J]. J Therm Anal Cal, 2005, 82(3): 671−675.
[24] BANJONG B. Kinetics and thermodynamic properties of the thermal decomposition of manganese dihydrogenphosphate dihydrate [J]. J Chem Eng Data, 2008, 53(7): 1533−1538.
[25] ANDREW K, GALWEY. Structure and order in thermal dehydrations of crystalline solids [J]. Thermochim Acta, 2000, 355(1−2): 181−238.

$La_2(CO_3)_3·3.4H_2O$ 在空气中热脱水的非等温动力学分析

张湘辉[1]，何 川[2]，汪 灵[1]，刘 菁[1]，邓 苗[1]，冯 谦[3]

1. 成都理工大学 材料与化学化工学院，成都 610059；
2. 中南大学 机电工程学院，长沙 410012；
3. 德国耐驰仪器制造有限公司 成都办事处，成都 610017

摘 要：采用水热法合成单相 $La_2(CO_3)_3·3.4H_2O$。采用 XRD、FTIR 以及 DTA−TG 对 $La_2(CO_3)_3·3.4H_2O$ 在 30~1000 °C 的热分解过程、中间及最终产物进行表征。在非等温条件下对 $La_2(CO_3)_3·3.4H_2O$ 在 30~366 °C 范围内的热脱水动力学进行研究。采用 Flynn−Wall−Ozawa 及 Friedman 等转化法计算其反应活化能并对其反应阶段进行分析。采用多元非线性回归程序确定其最可能的反应机理及动力学参数。结果表明，$La_2(CO_3)_3·3.4H_2O$ 的热脱水为三步竞争反应，一个 n 序列初始反应后为 n 序列竞争反应($F_nF_nF_n$ 机理)。经最可能的反应机理计算所得的活化能与 Friedman 等转化法的计算结果非常接近，拟合后的 TG 及 DTG 曲线与原始曲线能较好地吻合。

关键词：$La_2(CO_3)_3·3.4H_2O$；非等温动力学；同步热分析；脱水反应

(Edited by Hua YANG)